

BOND BEHAVIOR OF INDENTED WIRES IN PRETENSIONING

Stephan Geßner, Institute of Structural Concrete, RWTH Aachen University, Germany
Martin Henne, Ed. Züblin AG, Germany

ABSTRACT

The bond behavior of strands in pretensioned concrete members has been analyzed extensively in the past. Aside from strands, indented wires are also used for pretensioning in industry. Application areas of indented wires are, for example, concrete crossties and precast concrete poles. Due to the different shape and surface area, it can be expected that there is a difference in the anchorage mechanisms between strands and indented wires. Nevertheless, most studies on pretensioning only consider strands.

An experimental testing program has been conducted to determine the anchorage behavior of indented wires in pretensioned concrete elements. The program consists of pull-out tests and small-scale tests for transfer length measurement. Pull-out tests with varying transverse strain enable the simulation of local bond characteristics at different locations within the transfer length. In combination with the results from the transfer length measurement, constitutive equations for the bond properties of indented wires can be derived. Indented wires with different profiling are used in the program. The focus is on wires with very low indentation depths (about 0.1 mm or 0.0039 in). To get an approximate assessment for wires with very low indentation depth, some tests have been conducted with plain wires. In order to ensure comparability with results from the literature, 0.5'' strands have also been used in some tests. The paper presents the results of the experimental studies and ideas for the derivation of bond models.

Keywords: Pretensioning, Bond, Transfer length, Prestressing steel, Indented wires

INTRODUCTION

Prestressing is required for long spans, innovative floor systems, and economical girder designs. Usually, pretensioning is used for prefabricated concrete sections. For pretensioning, no anchorage devices are required as in post-tensioned members. Thus, the use of prestressing strands can be very cost-effective.

In the prestressing procedure, the required strands must first be pretensioned in a prestressing bed. After casting and hardening of the concrete, the pretensioning is released and transferred from the strand into the concrete. Here, no anchorage device is used and the stress is transferred by a bond. For this reason, the design must consider not only the moment and shear carrying capacity of the pretensioned beams, but the bond must also be guaranteed in order to prevent premature failure.

The bond behavior of strands in pretensioned concrete members has been analyzed extensively in the past. Aside from strands, indented wires are also used for pretensioning in industry. Application areas of indented wires are, for example, concrete crossties and precast concrete poles. Due to the different shape and surface area, it can be expected that there is a difference in the anchorage mechanisms between strands and indented wires. Nevertheless, most studies on pretensioning only consider strands. In this context, the work of PETERMAN et al.^{1,2,3} must be mentioned for investigating the anchorage of indented wires in pretensioning.

The application of indented wires is not generally accepted in all codes and guidelines. Whereas Eurocode^{4,5} and Model Code 2010⁶ enable the application of indented wires for pretensioning and give appropriate design recommendations, ACI 318-14⁷ only refers to strands. In the context of European standardization, a new norm for prestressing steel, FprEN 10138-2⁸, is in preparation. It will allow the use of indented wires, whose profiling is outside the field of experience of German regulatory authorities (DIBt); in particular, the indentation depth according to FprEN 10138-2 is much smaller than in currently used indented wires (0.1 mm instead of 0.2 mm, or 0.0039 in instead of 0.0078 in). For this reason, an experimental testing program is conducted to determine the bond behavior of indented wires with small indentation depths for pretensioning.

BOND MECHANISMS

BOND OF REINFORCING BARS

According to LEONHARDT⁹, bonding resistance between steel and concrete in RC structures consists of a combination of three components: adhesion, friction and mechanical anchorage. These components do not exclude each other; instead, they act according to the loading and surface conditions, simultaneously or successively.

In the contact zone between the concrete and steel, adhesion and capillary forces occur. This bond arises from the hardening of the concrete. The quality of adhesion is mainly determined by the surface conditions of the steel and on the properties of the hardened cement paste. The adhesive effect fails even at small relative displacements between the concrete and steel, and friction comes into effect as an additional bond mechanism. For this reason, adhesion is of minor importance for the bond behavior and is practically negligible.

Friction is based on forces in the contact zone between the steel and concrete. To activate frictional effects, force components acting perpendicularly to the contact surface are required. In general, the lateral pressure is given by external loads and expansion or shrinkage of the concrete. In addition to the level of the lateral pressure, the decisive factors for the amount of friction are roughness of the steel surface and the concrete composition. Furthermore, lateral pressure can be further increased by two possible factors: jamming of detached cement grains between the steel and concrete and the so-called "lack of fit". The "lack of fit" is caused by irregularities in the steel cross-section, whereby the steel does not fit into the concrete channel when slipping. Through these effects, friction correlates with the displacement between the concrete and prestressing tendon.

Mechanical anchorage (also known as shearing bond), which is the dominant bond mechanism in ribbed bars, derives from the contact between the rib and the surrounding concrete matrix. The ribs of the steel bars form a mechanical interlock between the steel surface and surrounding concrete, which enables significantly improved anchorage of the bar in the concrete, restricting the relative displacement of the elements. To activate the mechanical anchorage, a relative displacement between the steel and concrete, and, hence, internal cracking in the concrete are required. This glide path between the steel and concrete in the boundary layer is often referred to as slip. The mechanical interlock may occur through special design (ribbing, profiling) or by the natural roughness of the steel surface. The forces are transferred from the inclined rib flanks to the surrounding concrete (Fig. 1).

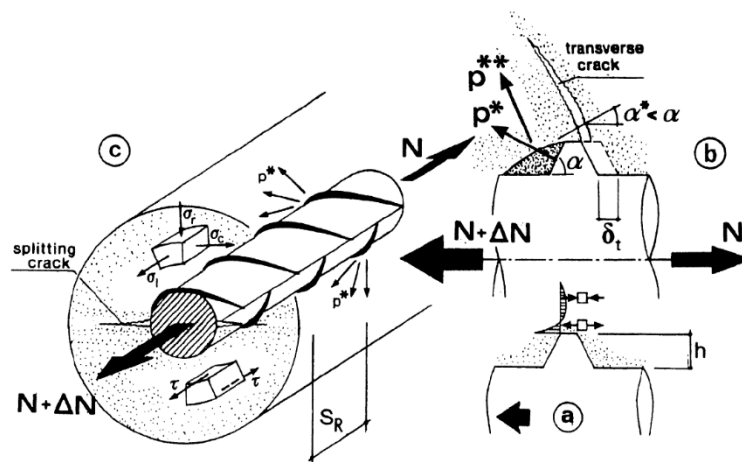


Fig. 1 Schematic view of the load transfer via mechanical anchorage¹⁰

The deformation behavior and the shear capacity of the concrete mortar in the bonding joint have a decisive influence on the level of mechanical anchorage. To shear off the concrete corbels between the ribs, large forces are necessary. Their carrying capacity and failure mode depend on the state of stress that develops in the mortar corbel (Fig. 2).

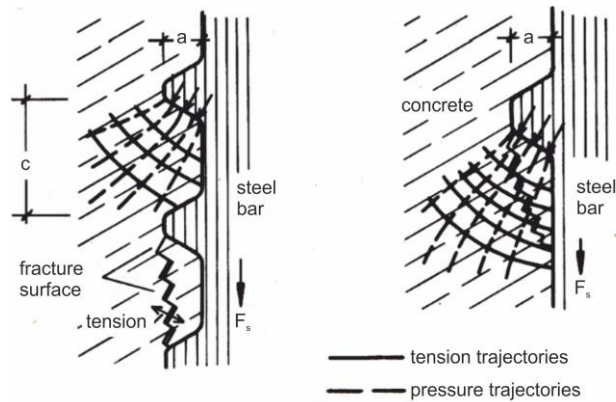


Fig. 2 Stress trajectories and fracture path with small (left) and large (right) rib spacing¹¹

According to REHM¹², the distribution of stresses correlates with the ratio of the rib's height (Fig. 2, a) to the rib spacing (Fig. 2, c). REHM and other researchers use the relative rib area (f_r) as a decisive factor for the characterization of the bond behavior of reinforcing steel. In general, the relative rib area is given as a quotient between the projected vertical area of the rib and the lateral area of the steel bar contained between two adjacent ribs.

The ribs are loaded by local stresses at high pressures. This loading creates a circular tensile stress condition in the concrete. When the spatial tensile stresses exceed the tensile strength of the concrete, longitudinal cracks occur. The tendency toward longitudinal cracking increases with the strength of the bond, as the forces have to be transferred within a short transfer length. To avoid sudden longitudinal cracks, a minimum concrete cover has to be ensured¹³.

BOND IN PRETENSIONING

For bond mechanisms in pretensioning, a distinction must be made between strands and indented wires.

The bond mechanisms of prestressing strands differ from those of conventional ribbed bars, in which the bond is based mainly on the shear forces between the concrete and the ribs. The bond for strands used in pretensioning is established by adhesion and friction. In order to obtain frictional forces, lateral stresses between the tendon and concrete are required. When the prestressing is released in the prestressing bed, the tendon tries to return to its unstressed state. The hardened concrete, however, counteracts this expansion, thus generating lateral pressure. This so-called "Hoyer effect," also known as wedge action, governs the bond strength of the strands (Fig. 3).

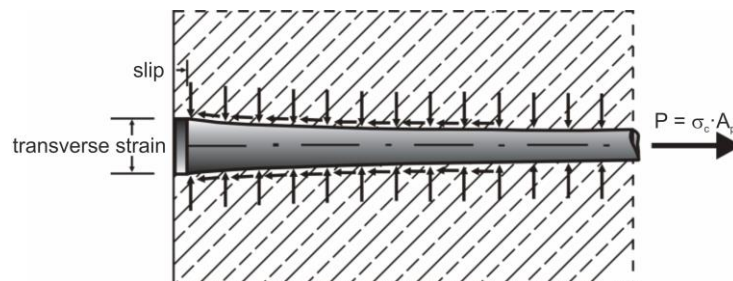


Fig. 3 The Hoyer effect¹⁴

Of course, the radial stresses also lead to tensile stresses in the surrounding concrete. If these stresses exceed the tensile strength, longitudinal cracks arise in the anchorage zone and the Hoyer effect disappears. For this reason, a sufficient concrete quality and concrete cover must be maintained, and lateral reinforcement may need to be applied accordingly.

The bond behavior of indented wires can be seen as a combination of the behaviors exhibited by strands and conventional ribbed bars. Aside from adhesion and friction due to the Hoyer effect, mechanical anchorage created by the indentations is also of importance.

Generally, the bond strength of tendons in pretensioning can be divided into three parts¹⁵:

- a constant part caused by basic friction, also called the rigid-plastic bond behavior;
- a stress-dependent part, which is based on the Hoyer effect and increases with the degree of prestressing;
- and a slip-dependent part, which is independent of prestressing. For strands, this effect can be explained by the “lack of fit” resulting from the geometry of the strands, which is not completely uniform. For indented wires, the influence of the mechanical locking by the profiling is crucial.

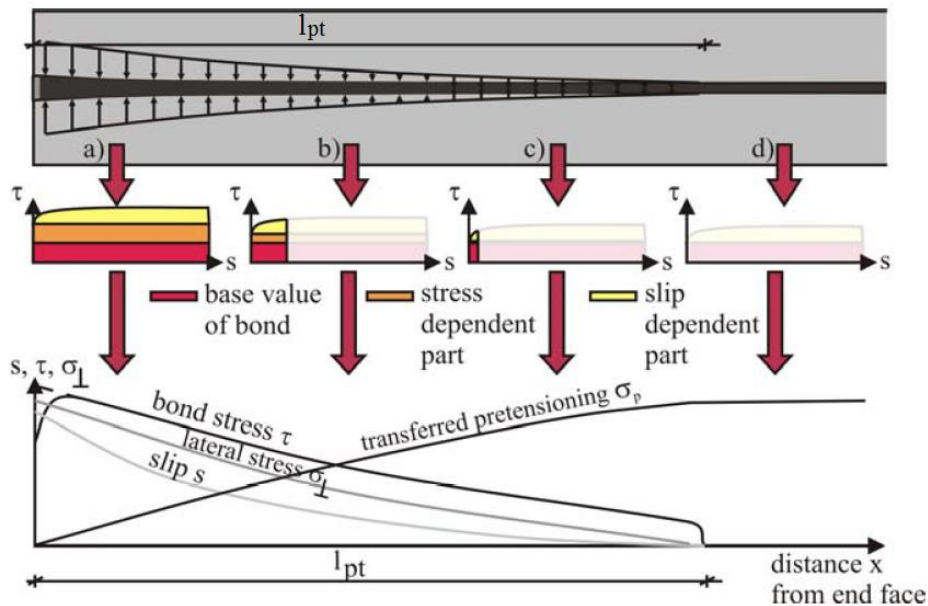


Fig. 4 Transfer of prestressing¹⁶

Figure 4 illustrates the principle of the transfer of prestressing. Both the lateral pressure and the slip decrease along the transfer length (l_{pt}) according to the prestressing of the strand, which has to be transferred into the concrete. Close to the concrete end face, almost the full prestressing has to be transferred, leading to high lateral pressure between the steel and concrete. All three bond components are fully activated. The prestressing of the concrete increases along the transfer length and, consequently, the stress that has to be transferred decreases. At the end of the transfer length (Fig. 4, c), most stresses have already been transferred from the steel to the concrete. Here, the

lateral stresses and the slip are very small; the bond is mainly established by the base value of the bond. Outside of the transfer length, there is neither bond nor lateral stresses nor slip due to prestressing.

EXPERIMENTAL INVESTIGATION

To investigate the bond behavior of indented wires in pretensioning, 108 pull-out tests and 25 small-scale beam tests were performed.

MATERIAL CHARACTERIZATION

The focus of the experimental investigations is on indented wires with very low indentation depths. Therefore, three types of indented wires with small indentation depths were investigated (Tendon no. 3, 4 and 5). All indented wires have a comparable relative rib area; however, they vary in profiling, nominal diameter, and steel grade.

In order to get a limit value range for very low indentation depths, some tests were done with smooth wires (Tendon no. 1 and 2). Since most research on the bond behavior in pretensioning concentrates on strands, tests with 7-wire 0.5" strands were used to make the results comparable with those for indented wires. The main tendon parameters are given in Table 1.

Table 1: Characterization of tendons

No.	Surface	Nominal diameter [mm (in)]	Indentation depth a [mm (in)]	Indentation spacing c [mm (in)]	Relative rib area f_r	Classification in accordance with FprEN 10138 ⁸	Steel grade $f_{pk}/f_{p0.2k}$ [MPa]
1		7 (0.28)	-	-	-	-	1570/1770
2		8 (0.31)	-	-	-	-	1570/1770
3		9.5 (0.37)	0.10 (0.0039)	5.8 (0.23)	0.014	T2	1375/1570
4		10.5 (0.41)	0.09 (0.0035)	5.8 (0.23)	0.013	T2	1375/1570
5		7.5 (0.3)	0.15 (0.0059)	8.1 (0.32)	0.014	T1	1470/1670
6		12.5 (0.5)	-	-	-	-	1570/1770

Two concrete compositions were used for the tests. The target values for the compression strengths for the two concrete materials are 25 MPa (3630 lbf/in²) and 50 MPa (7250 lbf/in²), tested on cylinders (D = 15 cm (5.9 in), h = 30 cm (11.8 in)) after two days of curing. The cement used for both mixtures is of the same strength class: CEM 52.5 R. The water/cement ratios were 0.625 and 0.353, no plasticizer was used, and the maximum aggregate diameter was 16 mm (0.63 in). The compositions of the concrete are given in Table 2.

Table 2: Concrete compositions

		Composition 1	Composition 2
Strength classification according to Eurocode ⁴		C30/37	C60/75
Cement CEM I 52,5R	[kg/m ³ (lb/ft ³)]	285 (17.79)	450 (28.09)
Grain classes [mm / in]:			
0 - 0,2 / 0 - 0.008	[kg/m ³ (lb/ft ³)]	173 (10.80)	165 (10.30)
0,2 - 1 / 0.008 - 0.039	[kg/m ³ (lb/ft ³)]	443 (27.66)	423 (26.41)
1 - 2 / 0.039 - 0.078	[kg/m ³ (lb/ft ³)]	193 (12.05)	184 (11.49)
2 - 4 / 0.078 - 0.156	[kg/m ³ (lb/ft ³)]	270 (16.86)	257 (16.04)
5 - 8 / 0.19 - 0.31	[kg/m ³ (lb/ft ³)]	385 (20.03)	367 (22.91)
8-16 / 0.31 - 0.63	[kg/m ³ (lb/ft ³)]	463 (28.90)	441 (27.53)
Water	[kg/m ³ (lb/ft ³)]	178 (11.11)	159 (9.93)
Water/cement ratio		0.625	0.353

PULL-OUT TESTS

A total of 108 tests were performed. The test parameters were the tendon profiling and the concrete strength. The testing setup was chosen in accordance with RILEM¹⁷ and NITSCH¹⁵.

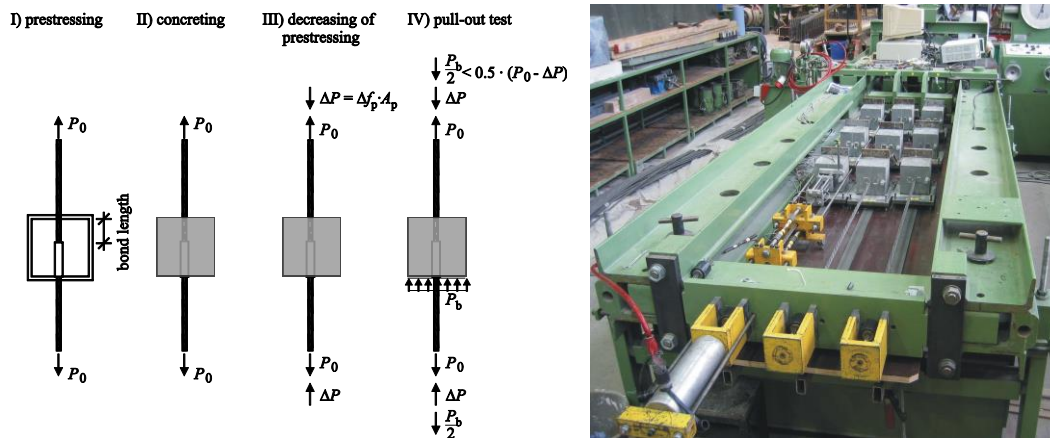


Fig. 5 Fabrication and test sequences of the pull-out tests and test rig

The edge length of the square specimens is 150 mm (5.9 in). The tendons were placed centrally in all tests so that the influence of the concrete cover is excluded. Due to the varying nominal diameters within the testing program, the embedment lengths were determined to be $l_b = 5 \cdot d_p$. Each test batch, consisting of a total of 9 tests, included three times three tests with different lateral strain stages (0 %, 50 %, 100 %). Here, 100 % means, for example with tendon no. 2 or no. 6, a change in the prestressing stress of $\Delta\sigma_p = 1275$ MPa (185,000 psi), 50 % means $\Delta\sigma_p = 637.5$ MPa (92,500 psi), and 0 % indicates no change. Figure 5 shows the sequences of the pull-out tests. Three tendons have been prestressed inside a rig (Fig. 5 right) before casting with the maximum allowed initial prestressing stress, $\sigma_{pm0} = \min \{0.75 \cdot f_{pk}; 0.85 \cdot f_{p01,k}\} = 0.85 \cdot 1500 = 1275$ MPa ($P_0 = \sigma_{pm0} \cdot A_p$), according to Eurocode^{4,5}. After two days, the first three tests were carried out. Afterwards, the prestressing force was decreased by about 50 % and the next three tests were performed. Finally, the last tests were carried out with full release

(100 %), which signifies a nearly full lateral strain of the strand. A small remaining force was needed to avoid the total relaxation of the strands on one side while increasing the bond forces ($P_b/2$ on each side in Fig. 5, phase IV).

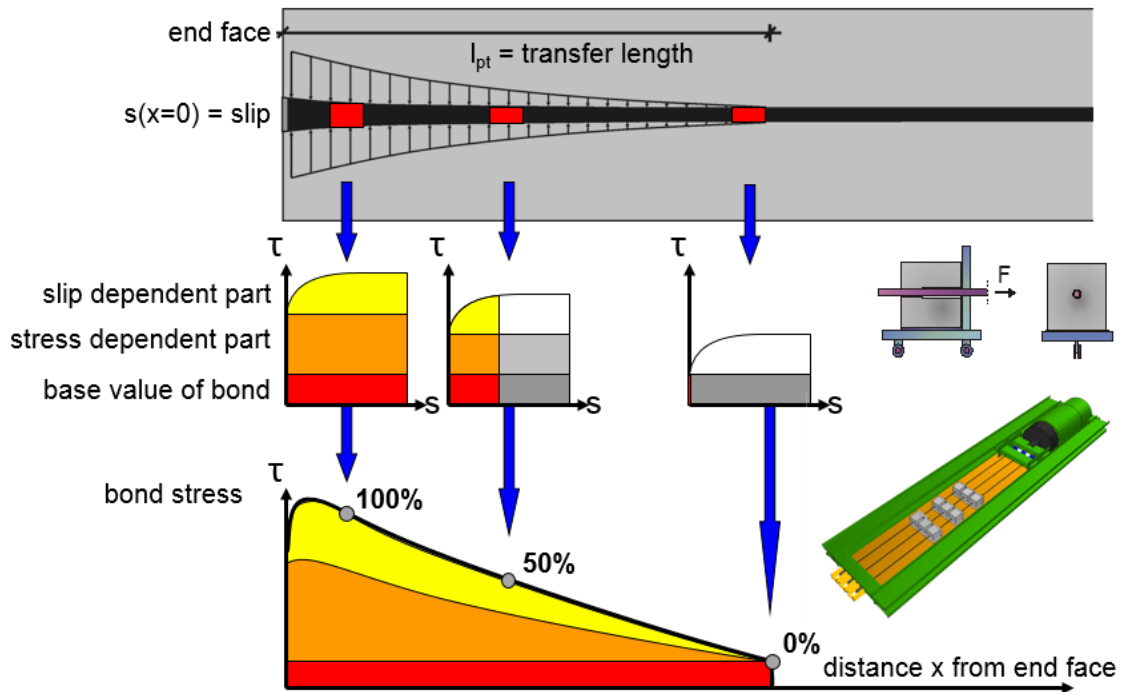


Fig. 6 Experimental set-up of the pull-out-tests

The bond stress τ_m was calculated with the nominal strand diameter, d_p :

$$\tau_m = \frac{P_p}{\pi \cdot d_p \cdot l_b} \tag{1}$$

where

P_b = bond force ($\sigma_p \cdot A_p$)

l_b = bond length

d_p = nominal tendon diameter

During the experimental procedure, the slip of the tendon is measured with inductive displacement transducers (IWA). The prestressing force is recorded continuously with load cells and strain gauges during the test procedure. For the analysis of the tests, bond stress-slip-diagrams are plotted. An overview of the conducted pull-out tests is given in Table 3.

Table 3: Overview of pull-out tests

Batch no.	Prestressing tendon			Concrete composition
	Tendon no.	Surface	Nominal diameter d_p [mm (in)]	
1	1	smooth	7 (0.28)	1
2	2	smooth	8 (0.31)	1
3	3	profiled	9.5 (0.37)	1
4	4	profiled	10.5 (0.41)	1
5	2	smooth	8 (0.31)	2
6	3	profiled	9.5 (0.37)	2
7	4	profiled	10.5 (0.41)	2
8	1	smooth	7 (0.28)	2
9	5	profiled	7.5 (0.3)	2
10	5	profiled	7.5 (0.3)	1
11	6	0.5" strand	12.5 (0.5)	1
12	6	0.5" strand	12.5 (0.5)	2

SMALL-SCALE BEAM TESTS

The transfer length was determined experimentally on small-scale beam tests ($l = 5.2$ ft). The test parameters were the tendon profiling, concrete strength, and the specific concrete cover. To administer different concrete covers, the prestressing was induced into beams with different cross-sectional dimensions. The initial concrete cover was chosen in accordance with Eurocode^{4,5}, with $c = 2.5 \cdot d_p$. Generally, this concrete cover is very small for indented wires; technical approvals of DIBt (German regulatory authority) specify a minimum concrete cover for indented wires of 40-50 mm (1.57-1.97 in) depending on the concrete strength. In case of bond failure, the test was repeated with an increased concrete cover of $c = 3.5 \cdot d_p$.

Two days after concreting, the prestressing force was released in a stepwise fashion. During these tests, the end slip and the concrete strains were measured. However, local bond stresses cannot be measured. In order to avoid any impact on the cracking, no stirrups have been installed in the specimens.

The 25 small-scale beam tests conducted were focused on two main targets:

- Evaluation of the transfer length and end slip of the specimen. Due to the induced prestressing, the members are shortened. The transfer length can be evaluated from the measured concrete strains along the specimens.
- The concrete cover as well as the spacing were varied to determine the minimum dimensions to transfer the prestressing without splitting cracks.

An overview of the conducted small-scale tests is given in Table 4.

Table 4: Overview small-scale tests

Test no.	Prestressing tendon			Concrete composition	Concrete cover c
	Tendon no.	Surface	Nominal diameter d_p [mm (in)]		
1, 2	2	smooth	8 (0.31)	1	$2.5 \cdot d_p$
3	5	profiled	7.5 (0.3)	1	$2.5 \cdot d_p$
4, 5	5	profiled	7.5 (0.3)	1	$3.5 \cdot d_p$
6, 7	4	profiled	10.5 (0.41)	1	$2.5 \cdot d_p$
8, 9	6	0.5" strand	12.5 (0.5)	1	$2.5 \cdot d_p$
10, 11	4	profiled	10.5 (0.41)	1	$3.5 \cdot d_p$
12, 13	2	smooth	8 (0.31)	2	$2.5 \cdot d_p$
14, 15	4	profiled	10.5 (0.41)	2	$2.5 \cdot d_p$
16, 17	4	profiled	10.5 (0.41)	2	$3.5 \cdot d_p$
18, 19	5	profiled	7.5 (0.3)	2	$2.5 \cdot d_p$
20, 21	5	profiled	7.5 (0.3)	2	$3.5 \cdot d_p$
22, 23	6	0.5" strand	12.5 (0.5)	2	$2.5 \cdot d_p$
24, 25	2	smooth	8 (0.31)	1	$2.5 \cdot d_p$

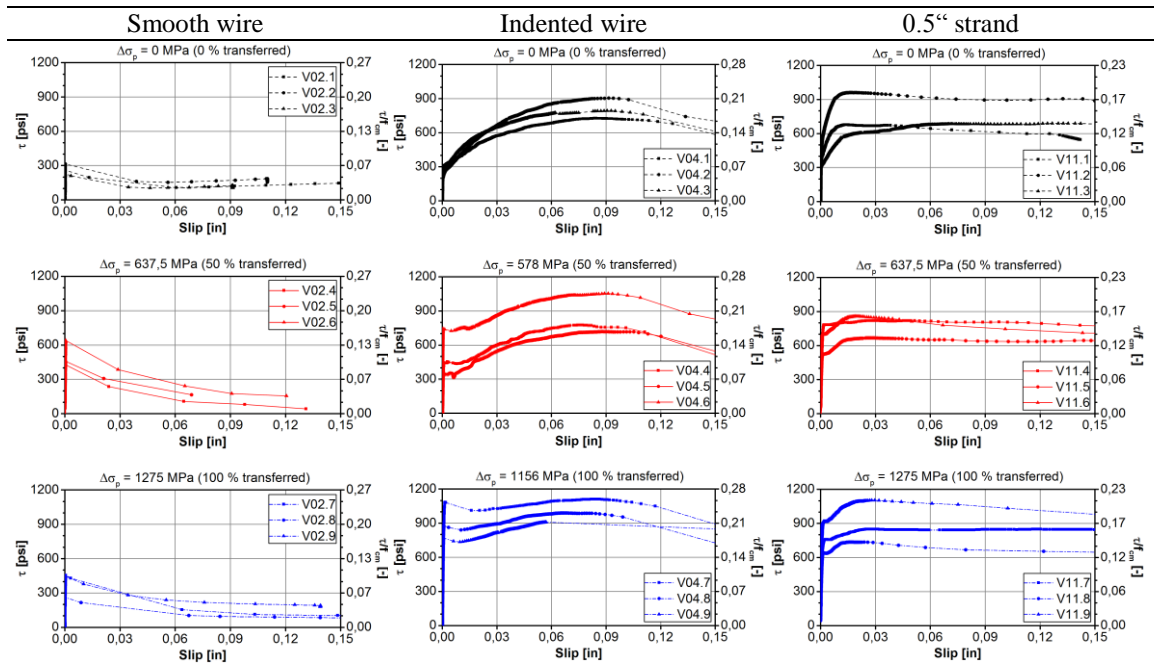
The analysis of the concrete strains was done with the methods given in RUSSEL¹⁸ (Average Maximum Strain Method) and WÖLFEL¹⁹ (DIBt-Method). Subsequently, the mean bond strengths were calculated with the transfer lengths and the measured prestressing forces (equation 1).

RESULTS

PULL-OUT TESTS

The results of the pull-out tests are shown in τ -s-diagrams (bond strength versus slip). The different bond behavior of the tendons is shown in the following diagrams. To demonstrate the fundamental differences between the bond behavior of smooth wires, indented wires, and strands, Table 5 shows the bond behavior at different prestressing force release states in normal strength concrete (composition 1).

Table 5: Characteristic results of pull-out tests



By transferring the prestressing force, the bond stresses can be increased significantly in the range of small displacements. In all the graphs, the Hoyer effect can be observed. The τ -s diagrams without released prestressing force ($\Delta\sigma = 0\%$) have a constant base value in the region of very small displacements. Compared to the tests with wires, the experiments with strands have higher base values. In contrast to the base value and the stress-dependent component, the slip-dependent component of the tendons differs fundamentally.

In the tests with smooth wires (Table 5, left), bond failure occurred after very low displacements. The slip-dependent bond behavior is significantly altered by the profiling (Table 5, center). The bond stresses increase up to a displacement of approximately 2 mm (0.078 in). After exceeding this maximum ($s \approx 2$ mm), bond failure occurs, as can be recognized by the decreasing density of the data points in the diagrams.

The slip-dependent bond behavior of strands exhibits a large increase in bond stresses in the range of slip smaller than 1 mm (0.039 in) (Table 5, right). At higher displacements, the bond stresses stay on a nearly constant level. Basically, the maximum bond stress can be increased only slightly by the release of the prestressing force. In contrast, the release of the prestressing force increases the bond stresses significantly for small slip.

SMALL-SCALE TESTS

In this test, the end slip and the concrete strains were measured. In Fig. 7, the transferred prestressing force is plotted against the measured end slip (top) and the concrete strain curve is shown along the small-scale girder (bottom). The left half of the figure shows an anchorage failure at 93 % release of the prestressing force, while the right half represents complete anchorage.

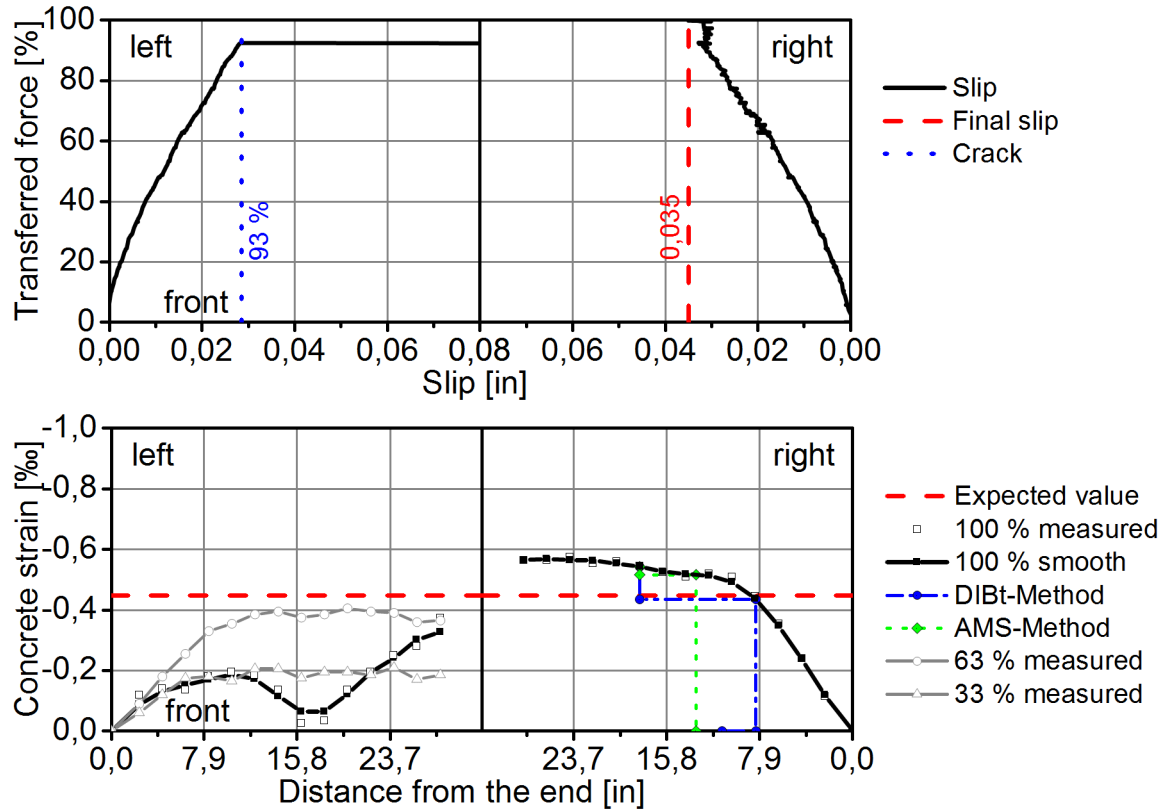


Fig. 7 Results of test no. 21

The transfer lengths are determined with the measured concrete strains. For a general comparison of the results, the transfer lengths are not suitable, since they are affected by the diameter of the prestressing steel and the material properties of both the prestressing steel and the concrete. In order to compare the results, a constant bond stress (τ_m) is calculated with equation (1) from the determined transmission length ($l_b = l_{pt}$).

In order to eliminate the influence of the concrete strength, the bond stresses are scaled by the mean compressive strength for the tests ($f_{cm, cube150, 2d}$) in Fig. 8.

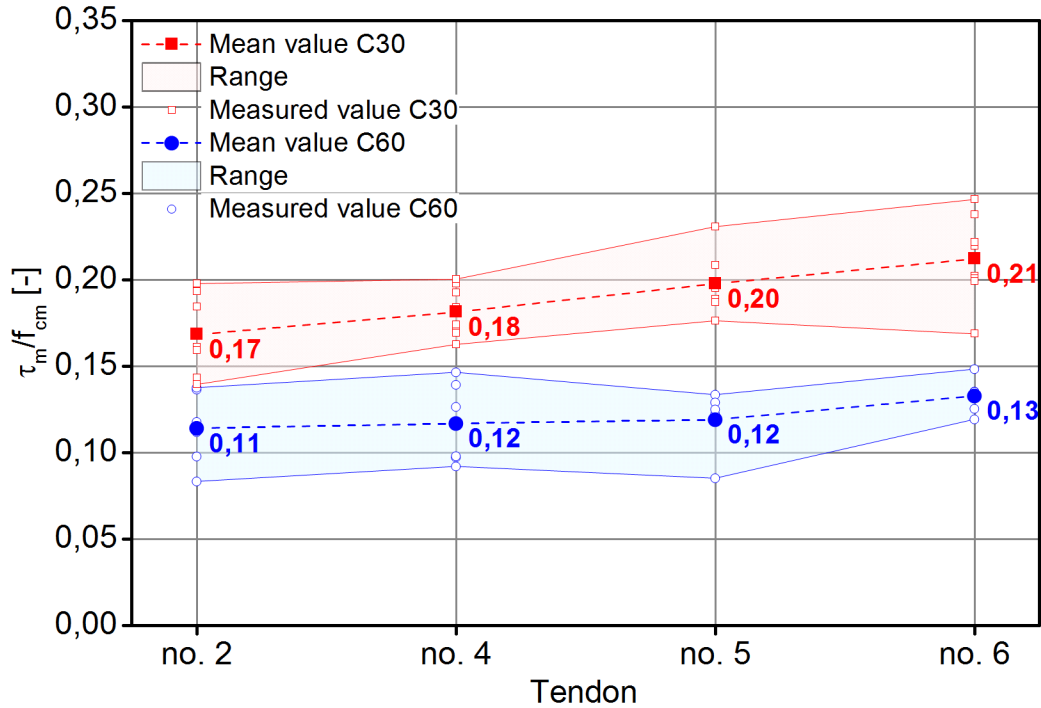


Fig. 8 Comparison with scaled bond stresses

The dimensionless value τ_m/f_{cm} (bond stress scaled by the mean compressive strength) enables the comparison of the transfer lengths and an interpretation of the bond behavior of the tendons (Fig. 8). As expected, the smooth wire (tendon no. 2) has the lowest scaled mean bond stresses. Profiling improves the performance of the bond behavior; tendon no. 4 and tendon no. 5 have higher bond stress values. The highest scaled mean bond stress is achieved with strands. Furthermore, it can be stated that the bond strength does not increase linearly with the concrete compressive strength, as the scaled values of concrete composition 2 are lower than those of composition 1.

In addition to transfer lengths and bond stresses, the minimum concrete cover was also examined in the small-scale tests. In the tests with smooth wires (tendon no. 2) and strands (tendon no. 6), the prestressing force could be transferred without cracking, while the scaled concrete cover was $c/d_p = 2.5$. In contrast, many tests with indented wires failed due to longitudinal cracking in the anchorage area (Table 6), even though the scaled concrete cover was increased in some tests to $c/d_p = 3.5$. Furthermore, the cracking behaviors of the tests with tendons no. 4 and no. 5 differ from each other. While in ribbed reinforcing bars, the relative rib area (f_r) contains great informational value on the bond behavior, the tested indented wires with low indentation depths behave differently in pretensioning despite the comparable relative rib area.

Table 6: Number of failed anchorages

	Tendon no. 4		Tendon no. 5	
	Composition 1	Composition 2	Composition 1	Composition 2
$c/d_p = 2,5$	7/8	1/8	4/4	5/8
$c/d_p = 3,5$	0/7	0/8	2/8	2/8

By using higher concrete strengths (which involves higher bond strength) and/or larger concrete covers, the incidence of longitudinal cracks can be reduced. It is striking that tendon no. 5, compared to tendon no. 4, has a significantly higher risk of cracking in the anchorage area (cf. Table 6). The reason for this contrast is the different profiling. The indentation depth of tendon no. 5 is 0.15 mm (0.0059 in), whereas the indentation depth of tendon no. 4 ($a = 0.09$ mm i.e. 0.0035 in) is significantly lower. Since both tendons have nearly equal relative rib areas, the indentation spacing in tendon no. 5 ($c = 8.1$ mm i.e. 0.32 in) is significantly greater (about 5.8 mm i.e. 0.23 in in tendon no. 4). The load of the mortar corbels differs due to the adapting state of stress. REHM's¹² presumption that a wide rib spacing (or large indentation spacing) and high corbels (or large indentation depths) result in a higher risk of longitudinal cracking also applies to indented prestressing wires with low indentation depths. Furthermore, it can be stated with reference to the test evaluation (Fig. 7) that an increase in the relative concrete cover to $c/d_p = 4.0$ is probably sufficient for the crack-free transfer of the prestressing force.

DERIVATION OF BOND LAWS

The test results show that a classification through three bond components as proposed by NITSCH¹⁵ is applicable for the description of bonds in pretensioning. Below, the basic steps for the derivation of bond laws are briefly outlined. The bond τ results from summing the three bond components determined in the pull-out tests:

$$\tau = \tau_A + \tau_B + \tau_C \quad (2)$$

where

τ_A = base component

τ_B = stress-dependent component

τ_C = slip-dependent component

In Fig. 9, the bond components are presented in τ -s diagrams according to the results of the pull-out tests.

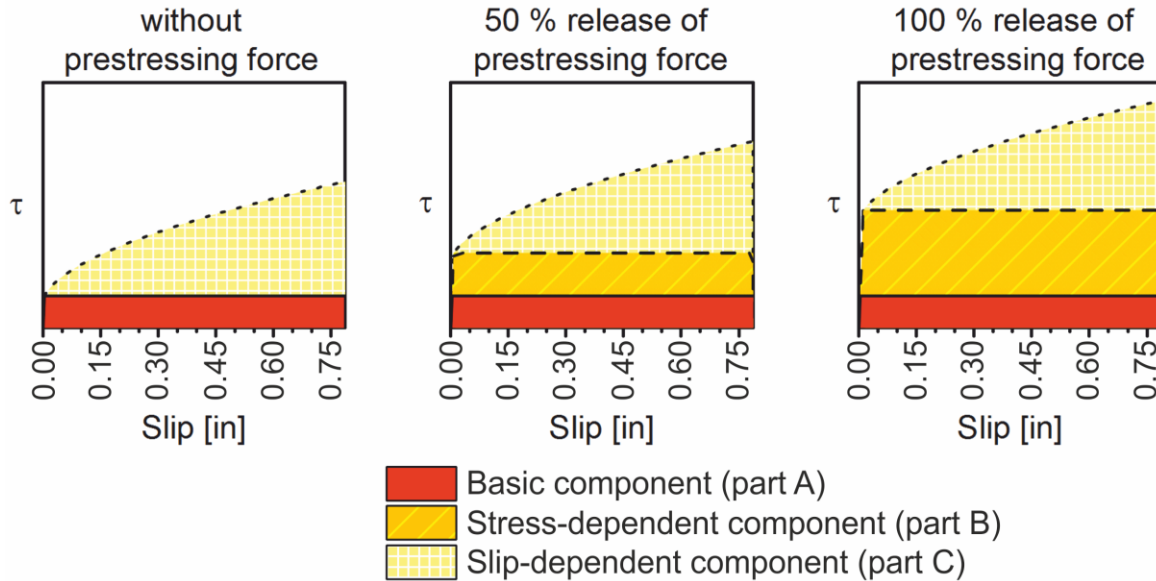


Fig. 9 Schema of bond components without and with release of prestressing force

Based on the results of 108 pull-out tests, a consistent method for the determination of the bond components was developed²⁰.

First, the base component (part A) is identified by regarding the pull-out test without release of prestressing force (Fig. 9, left). Generally, part A is assumed to be constant. By surveying the τ -s diagrams in the range of very small displacements, it can be seen that the base value is reached after very small slip. The base part is thus methodically defined as the value of the bond at a slip of 0.01 mm (0.004 in).

To determine the stress-dependent component (part B), the results of the pull-out tests with release of the prestressing force are used (Fig. 9, center and right), as the stress-dependent component correlates with the released prestressing force. The test results show that the slip-dependent component (part C) is negligible for small displacements; hence, the stress-dependent part can be calculated by subtracting part A from the total value of the bond. As with part A, surveying the τ -s diagrams in the range of very small displacements indicates that part B is reached after very small slip. To establish an evaluation method, the test results indicate that the bond value at a slip of 0.05 mm (0.002 in) is of sufficient accuracy (c.f. Fig. 10).

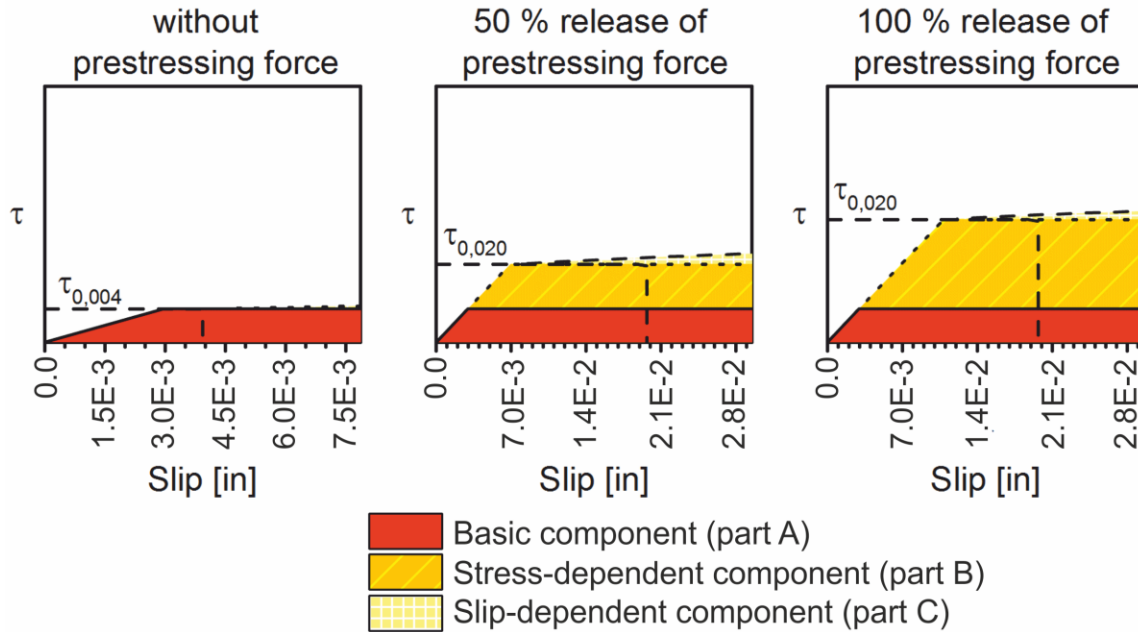


Fig. 10 Schema of bond components without and with release of prestressing force in the range of very small displacements

To determine the slip-dependent component (part C), only the area with slip less than or equal to 2.0 mm (0.079 in) is considered (Fig. 11). This simplification is justified by the fact that the tendon slip reached in the small-scale tests was smaller than this limit. Experimental investigations have shown that the transferred prestressing force has only a small influence on the maximum bond strength of indented wires (cf. Table 5), whereas it significantly affects the value of the bond when the slip is very small (Fig. 11).

Part A and part B have considerable influence on the curve progression in the area of very small displacements. In the mathematical model, a power function is used for part C, which is dependent upon the transferred prestressing force and the concrete compressive strength. The power function is adapted numerically such that its results differ only slightly with the results from the pull-out tests at a displacement of 2.0 mm (0.079 in).

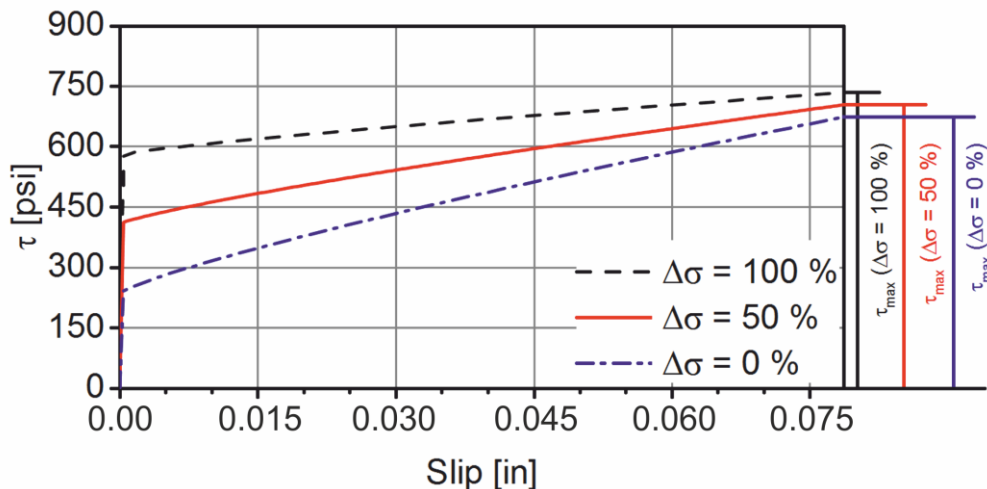


Fig. 11 Schema for the determination of bond strength curves

The results (slip and transfer length) of the small-scale tests are recalculated analytically by using a differential equation approach^{12,15,16,21,22}. The equation is solved with gradual integration; the differential equation approach uses the derived bond laws.

In Fig. 12 and Fig. 13, the results of the calculations are validated against the results of the small-scale tests. The derived bond laws for indented wires, smooth wires, and strands coincide well with experimental results.

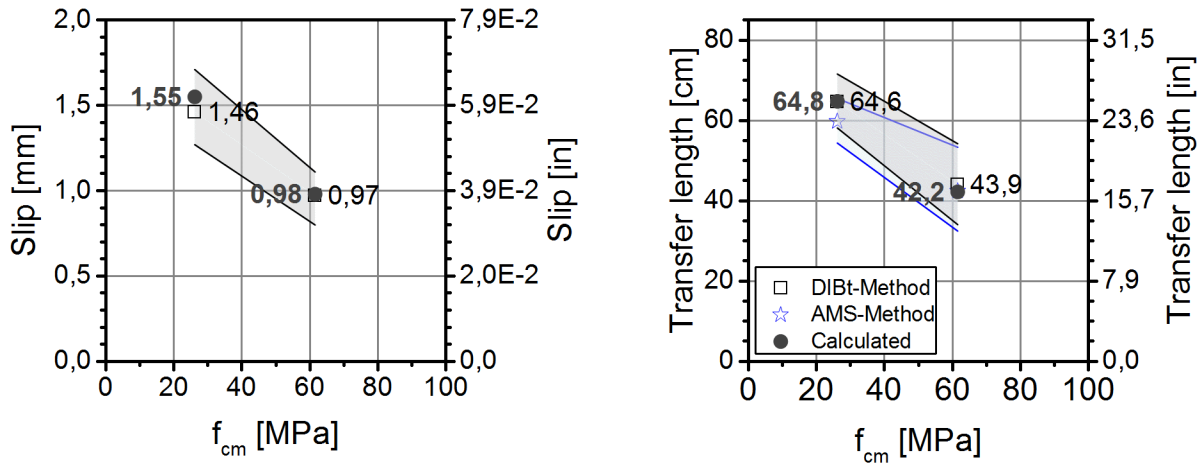


Fig. 12 Comparison of test results with numerical calculations (Tendon no. 4)

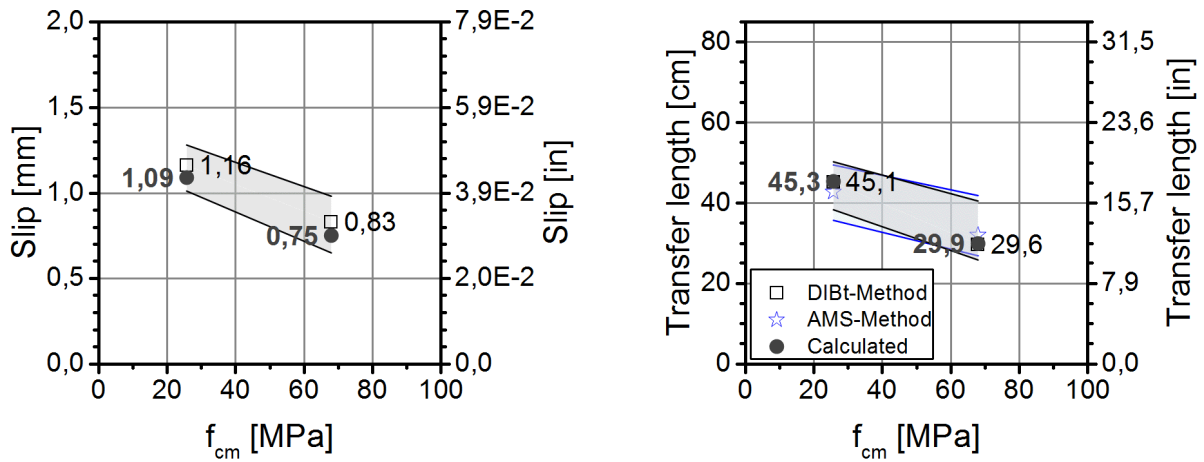


Fig. 13 Comparison of test results with numerical calculations (Tendon no. 5)

COMPARISON WITH CODES

In current codes such as ACI 318-14⁷, Eurocode^{4,5}, or Model Code 2010⁶, the approaches to calculate the transfer lengths and the bond stresses are distinctly different. For evaluation, all values according to the standards are used at a mean value level without factors of safety in order to compare the bond behavior realistically.

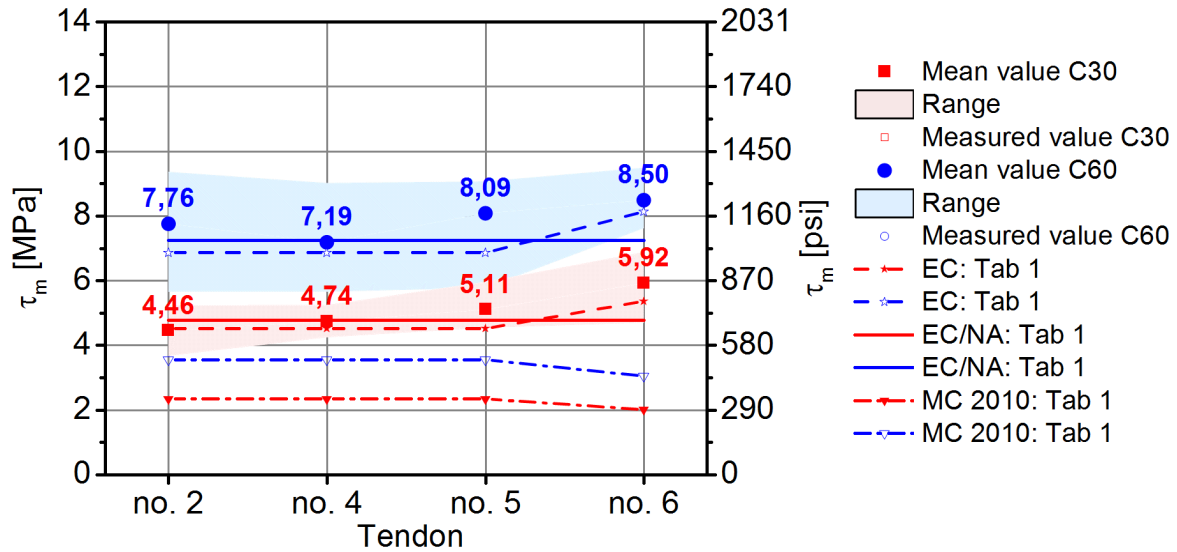


Fig. 14 Comparison of test results and codes on the basis of bond stresses

In Fig. 13, the mean bond stresses (τ_m) are given in accordance with Model Code 2010⁶ (MC), Eurocode⁴ (EC), and the German National Annex of Eurocode⁵ (EC/NA). They are compared with the results from the small-scale tests. ACI 318-14⁷ (ACI) is not taken into account, as it does not use bond strength values.

Generally, there is good agreement between the test results and the Eurocode values. The only difference between EC and EC/NA in the calculation of the mean bond stress is the factor η_{p1} . EC specifies $\eta_{p1} = 2.7$ for indented wires and $\eta_{p1} = 3.2$ for strands, whereas EC/NA ($\eta_{p1} = 2.85$) does not differentiate between indented wires and strands. For strands, the more progressive values of EC have better conformity with the testing results. The bond values of MC underestimate the testing results to a great extent. The lower bond stresses for strands compared to indented wires in MC are particularly divergent from the test results.

Using the calculated bond stresses, the transfer length can be determined. As the bond stresses according to EC and EC/NA differ, the transfer lengths for both codes are plotted in Fig. 15. When calculating the transfer length according to MC (which is referred to as the transmission length in MC), no formulas for the mean transfer length are given. The design value is determined through the factor α_{p2} depending on the loading situation. For a direct comparison at a mean value level, the extremes are averaged.

The dashed line in Fig. 15 is the transfer length according to ACI. The line is horizontal as the formula for the transfer length in ACI only depends on the tendon diameter.

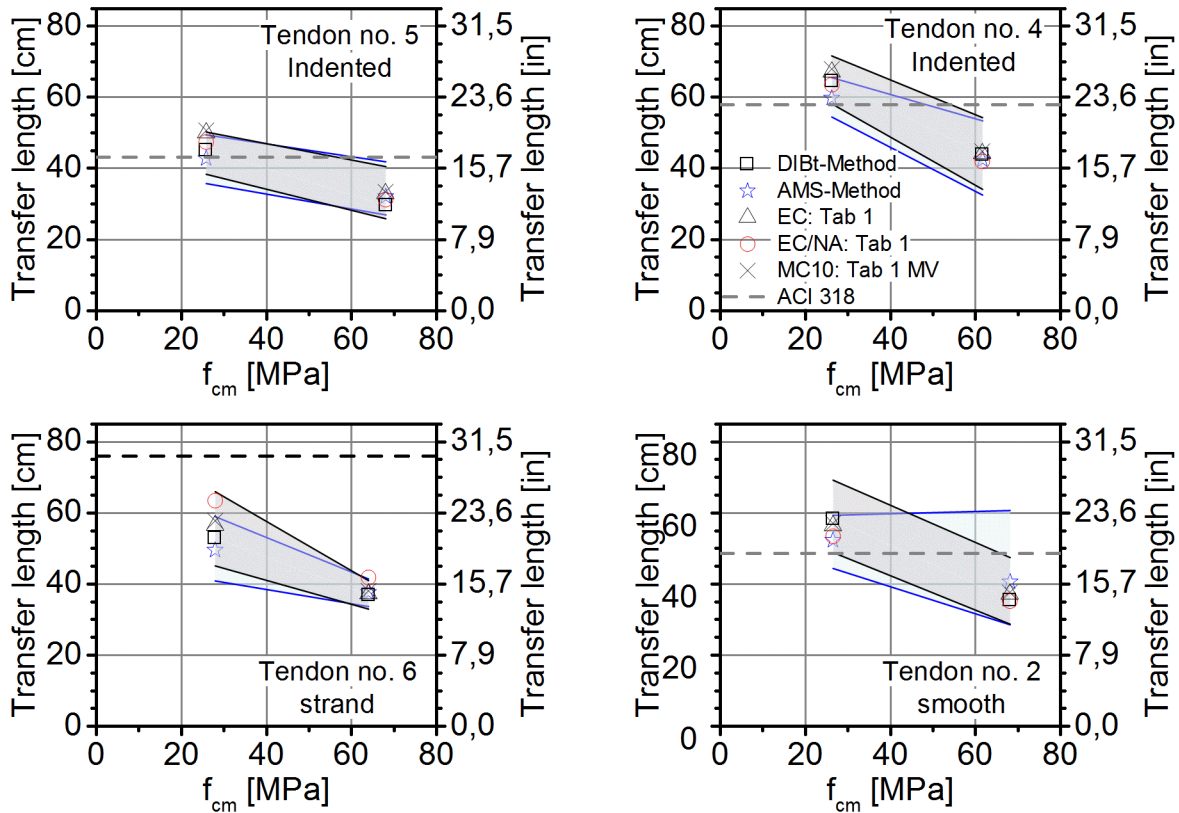


Fig. 15 Comparison of test results and codes on the basis of transfer lengths

The transfer lengths of EC show good correlation with the test results (Fig. 15). The differences between EC and EC/NA are minimal and come solely from the difference in the bond stress due to the parameter η_{p1} . In contrast to the comparison of bond stresses for MC, the results for transfer length calculations based on MC also correlate very well with the test results.

For the strands tested in this program (Fig. 15, lower left), the values referenced in ACI are conservative. Meanwhile, the test results for indented and smooth wires are not covered by the code. This is no surprise, as ACI only allows the application of strands.

On the basis of the work done, an adaptation of the existing design rules (excluding ACI) for indented wires with low indentation depths is not necessary. According to the test results, even smooth wires are able to fit within the design concepts of EC and MC; nevertheless, the application of smooth wires should be excluded, as their failure is brittle.

CONCLUSIONS

To investigate the bond behavior of indented wires with very low indentation depths in pretensioning, an extensive experimental program has been conducted.

The pull-out tests are used to characterize and distinguish the bond behavior of indented wires, smooth wires, and strands. Based on the results of the pull-out tests, it is possible to derive bond laws that consider different bond mechanisms and enable the prediction of the bond behavior, transfer length, and end slip.

Furthermore, 25 small-scale tests were carried out to determine the transfer length and end slip. The tests enable the comparison of the transfer lengths and bond stresses attained with the values from current design codes (Eurocode, Model Code 2010, ACI 318-14). In addition, the small-scale tests are used to check the minimum concrete cover and to verify the derived bond laws.

As a result, it could be shown that the bond behavior of indented wires differs from that of strands. The slip-dependent component is especially different due to mechanical anchorage. The formulas for transfer length in Eurocode and Model Code 2010 yield good results, whereas ACI 318-14 is not suitable for indented wires. A modification of the transfer length calculation in Eurocode for indented wires with very low indentation depths is not necessary. However, the minimum concrete cover in Eurocode is not sufficient for indented wires. For this purpose, a minimum scaled concrete cover of $c/d_p = 4.0$ is suggested.

REFERENCES

1. Bodapati N., Peterman R., Zhao W., Beck B., Wu J., Holste J., Arnold M., Benteman R., Schweiger R., Transfer-length measurements on concrete railroad ties fabricated with 15 different prestressing reinforcements, 2013 PCI Convention and National Bridge Conference, September 21-24, Grapevine, 2013.
2. Bodapati N., Zhao W., Peterman R., Wu J., Beck B., Haynes M., Holste J., Influence of Indented Wire Geometry and Concrete Parameters on the Transfer Length in Prestressed Concrete Crossties, Proceedings of 2013 Joint Rail Conference, April 15-18, 2013, Knoxville, USA.
3. Arnold M., Peterman R., Bodapati N., Beck B., Wu J., Development of a standard bond test for indented prestressing wires, Proceedings of 2013 Joint Rail Conference, April 15-18, 2013, Knoxville, USA.
4. DIN EN 1992-1-1, Eurocode 2: Design of concrete structures – Part 1-1: General rules and rules for buildings, 2010.
5. DIN EN 1992-1-1/NA, National Annex – Nationally determined parameters – Eurocode 2: Design of concrete structures – Part 1-1: General rules and rules for buildings, 2010.
6. fib Model Code for Concrete Structures 2010, International Federation for Structural Concrete (fib), Ernst & Sohn Verlag, Berlin, ISBN: 978-3-433-03061-5, October 2013.
7. ACI 318-14: Building Code Requirements for Structural Concrete and Commentary, ACI committee, ISBN: 978-0-870-31930-3, 2014.
8. FprEN 10138-2 Final Draft, European Standard, Prestressing steels - Part 2: Wire, August 2009 (not published).
9. Leonhardt F., On the need to consider the influence of lateral stresses on bond, RILEM: Symposium on Bond and Crack Formation in Reinforced Concrete, Stockholm, 1957, 29–34.
10. Bond of reinforcement in concrete - State-of-art report, International Federation for Structural Concrete (fib), Lausanne, 2000.
11. Trost H., Teilweise Vorspannung - Verbundfestigkeit von Spanngliedern und ihre Bedeutung für Rissbildung und Rissbreitenbeschränkung, Ernst, Berlin, 1980.

12. Rehm G., Über die Grundlagen des Verbundes zwischen Stahl und Beton, Deutscher Ausschuss für Stahlbeton, Heft 138, Berlin, 1961.
13. Martin H., Noakowski P., Verbundverhalten von Betonstählen, Untersuchung auf der Grundlage von Ausziehversuchen, Deutscher Ausschuss für Stahlbeton, Heft 319, Berlin, 1981.
14. Hoyer E., Der Stahlsaitenbeton - Bd I: Träger und Platten, Elsner, Berlin, 1939.
15. Nitsch A., Spannbetonfertigteile mit teilweiser Vorspannung aus hochfestem Beton, doctoral thesis, RWTH Aachen University, ISBN: 3-98073202-2-0, September 2001.
16. Bülte S., Verbundverhalten von Spannstahl mit sofortigem Verbund, doctoral thesis, RWTH Aachen University, ISBN: 3-939051-04-7, July 2008.
17. Rilem RC6 TC9-RC: Bond test for reinforcement steel. 2. Pull-out test, *Materials and Structures*, V.6, No.32, March-April 1973, Rilem Publications, 2nd edition May 1983.
18. Russel B.W., Burns N.H., Design guidelines for transfer, development and debonding of large diameter seven wire strands in pretensioned concrete girders. Research-Report 1210-5F, Austin: Center of Transportation Research, The University of Texas at Austin, 1993.
19. Wölfel E., Krüger F., Verbundverankerung von Spannstählen – Zulassungsprüfung und Anwendungsbedingungen. *Mitteilung IFBt*, No. 6/1980, June 1980, 174-177.
20. Henne M., Untersuchungen zum Verbundverhalten profilierter Spanndrähte, master thesis, RWTH Aachen University, 2015 (not published).
21. Empelmann M., Zum nichtlinearen Trag- und Verformungsverhalten von Stabtragwerken aus Konstruktionsbeton unter besonderer Berücksichtigung von Betriebsbeanspruchungen, doctoral thesis, RWTH Aachen University, ISBN:3-9804729-0-6, 1995.
22. Bertram G., Zum Verbund- und Querkraftverhalten von Spannbetonträgern aus ultrahochfestem Beton, doctoral thesis, RWTH Aachen University, ISBN: 3-939051-15-2, August 2012.